MODELLING OF CASSON FLUID FLOW THROUGH AN ANNULAR REGION AND ITS DUAL SOLUTIONS

Abstract

This study's goal is to examine the nature of dual solutions and their stability in the context of heat transfer phenomena in the magnetized Casson fluid flow through an annular gap. An uniform magnetic field is applied in the normal direction of the fluid flow. The suitable similarity transformation and the MATLAB routine bvp4c solver scheme are employed to solve the governing equations. To define stable and physically feasible solutions, the stability analysis is put to use. Graphical displays show the effects of non-dimensional factors on temperature and velocity distributions. Additionally, the Nusselt number and skin friction coefficient are examined in tabular form. Also, the skin friction coefficient and Nusselt number are scrutinized in tabular form. From the discussion, we have learned that the Casson fluid parameter and the Hartmann number accelerate the velocity of the fluid in different cases of present geometries. The Eckert number is used as a temperature enhancing parameter. From the results, we have found that dual solutions exist up to a certain region of the similarity variable, and the first solution is stable and physically tractable over the second solution.

Index Terms: Dual Solutions, MHD, Casson fluid, Heat transfer, Stability Analysis, Annular region.

Keywords: The suitable similarity transformation and the MATLAB routine bvp4c solver scheme are employed to solve the governing equations.

Author

Rupjyoti Borah
Department of Mathematics
Tingkhong College
Dibrugarh, Assam, India
rpjtbrh@gmail.com

I. INTRODUCTION

The significance of the non-Newtonian fluids (non-linear relationship between the shear stress and the rate of deformation) is due to their appropriate applications in the engineering sciences, industrial processes, medical sciences, etc., which are more advanced than the Newtonian fluid in recent times. The Casson fluid is a special kind of non-Newtonian fluid that needs a yield stress to express its constitutive equations, and it behaves like an elastic solid. This type of fluid flow has multiple realistic applications, such as food processing, bio-engineering operations, fuel cells, fiber technology, nuclear reactors, etc. Jelly, Tomato sauce, honey, human blood, etc. are some real life examples of Casson fluid. Again, the impact of the magnetic field on the fluid flow has been widely recognized by engineers and scientists because of the imperative applications such as MHD pumps, MHD horizontal multistage pumps, etc. Fluid motion over stretching or shrinking surfaces and the heat transfer phenomenon have many implications for several industrial processes. Also, the fluid flow through this present geometry has occurred in many practical technology-driven applications, such as the assembly of oil and gas, electrochemical cells, fluid viscometers, hydraulic equipment, etc.

Crane [1] was the first author to investigate the nature of fluid flow due to the stretching or shrinking surface. After that, a huge amount of research works of different fluids flow due to this type of geometries are available in different research areas from the several decades. In recent times, many authors (Tamoor *et al.* [2], Debnath *et al.* [3], Dey and Hazarika [4], and Mahdy and Ahmed [5]) have investigated the impact of MHD on boundary layer flows of different fluids. Nagaraju and Garvandha [6] have inspected the thermally stratified viscous fluid flow under the influence of a magnetic field through a circular pipe.

Krishna *et al.* [7] have put their ideas about the influence of chemically stratified MHD flow over stretching sheets. Okedayo *et al*. [8] have examined the MHD flow and the effects of heat transfer by accounting for a cylindrical pipe that is filled with porous medium. Eldesoky *et al*. [9] have investigated the effects of magnetic field and thermal transmission on fluid flow by using a catheterized wavy tube. Recently, Gireesha and Sindhu [10] have investigated the significance of MHD boundary layer flow through annular microchannels with porous medium. Barman *et al. [11*] have examined the fluid flow through the annular gap between the concentric cylinders and offered many practical applications related to this present model. Again, Eldesoky *et al.* [12] have investigated the interface between compressibility and particulate suspension in peristaltically constrained flow due to the planner channel. In recent years, many researchers, such as Shafee *et al.* [13], Ahmed *et al.* [14], and Ahmed *et al.* [15], have examined the flow behaviors within tubes and channel walls of different fluids, like hybrid nanofluids, micropolar fluids, etc. Sadaf and Abdelsalam [16] have investigated the characteristics of hybrid nanofluids with different flow parameters by considering the wavy, non-unoform annular region.

Due to the lack of information about the smoothness of the surface, length of the geometries, and shrinking and moving surfaces, some irregular behaviors of fluid flow are observed, which occur with the change of time. To control this type of instability in the flow, many researchers have spent their time with this type of problem and found two solutions: one that is dependent on time and another that is independent of time. Markin [17] was the first author to investigate the dual solutions and their stability. After that, many researchers

(Weidmann *et al. [18*], Zaib *et al.* [19], Adnan *et al. [20]*, Ishak *et al. [21]*, etc.) have investigated the stability analysis of the dual solutions of the Newtonian and non-Newtonian (Casson fluid, nanofluid, etc.) fluids with heat transfer due to the different surfaces and put the importance of these fluid models in the various scientific fields. In recent times, Dey and Borah [22, 23] have investigated the dual solutions of viscous fluid flow over an exponentially shrinking cylinder and their nature of flow. Mishra *et al. [24*] have investigated the hydromagnetic flow and its stability on the dual solutions over a stretching or shrinking surface.

This present work is all inspired by the above literature and its immense relevance in different physical fields. We have studied the MHD Casson fluid flow through an annular gap between the concentric cylinders by assisting the MATLAB routine bvp4c solver scheme. Due to the contracting surfaces of the outer/inner cylinders of this model, the existence of dual solutions and their stability analysis are investigated together with heat transfer phenomena. The results are discussed pictorially, and the stable and unstable flows are analyzed using the concept of the normal mode method. Based on our knowledge, we have confirmed that the dual (steady and unsteady) solutions and their stability analysis of this fluid model through the annular region of the concentric cylinders have not been established until now. From the literature review, we have seen that lots of studies have focused on various aspects of the topic or subject area, but none of them deal with this particular research idea. So, we are unable to compare our work with existing literature.

1. **Mathematical Formulation:** We have considered the hydro magnetic two-dimensional steady and incompressible Cass on fluid flow with heat transfer through an annulus. During the entrance part of the annular region, the flow is behaving like a boundary layer flow until it reaches to fully developed flow (where flow properties are independent of the direction of x). So, we mainly concentrate on the boundary layer region. The geometry of this present problem is shown in Fig.1. Here, we have considered the following three cases:
   - The inner cylinder of radius r_1 of this annulus characterized with the shrinking velocity $u_w = \frac{u_0 x}{l}$ such that the constant $u_0 < 0$ signifies shrink at the surface of the inner cylinder and T_0 the prescribed temperature at the surface,
   - The outer cylinder of radius r_2 characterised with the shrinking velocity $u_w = \frac{u_0 x}{l}$ with T_1 the surface temperature of the outer cylinder and
   - Both the cylinder are shrank at the respective surface.

The relationship of their radii and wall temperatures are given by $r_2 > r_1 \,\&\, T_0 > T_1$. An uniform magnetic field B_0 is applied in the transverse direction of the flow.

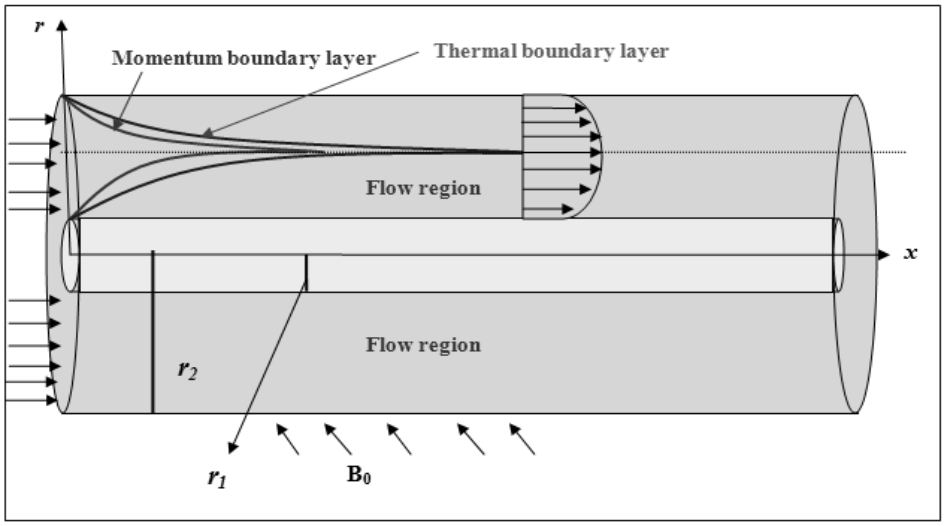

Figure 1: Flow Diagram

Following the theory of boundary layer approximations, the governing equations of this present problem are:

$$\frac{\partial(ru)}{\partial x}+\frac{\partial(rv)}{\partial r}=0, \tag{1}$$

$$u\frac{\partial u}{\partial x}+v\frac{\partial u}{\partial r}=\upsilon\left(1+\frac{1}{\beta}\right)\left(\frac{\partial^2 u}{\partial r^2}+\frac{1}{r}\frac{\partial u}{\partial r}\right)-\frac{\sigma {B_0}^2}{\rho}u, \tag{2}$$

$$u\frac{\partial T}{\partial x}+v\frac{\partial T}{\partial r}=\frac{k}{\rho C_p}\left(\frac{\partial^2 T}{\partial r^2}+\frac{1}{r}\frac{\partial T}{\partial r}\right)+\frac{\mu_\beta}{\rho C_p}(1+\frac{1}{\beta})\left(\frac{\partial u}{\partial r}\right)^2+\frac{\sigma {B_0}^2}{\rho C_p}u^2, \tag{3}$$

Where, $u\&v$ are the velocity components along the flow direction and radial direction respectively $\beta=\frac{\mu_\beta\sqrt{2\pi_c}}{P_y}$ is responsible for the Cas son fluid such that its value $\beta\to\infty$ represent the Newtonian fluid. $\upsilon,\rho,\sigma,C_P,k\&T$ Are the kinetic viscosity, density of the fluid, electrical conductivity, specific heat at constant pressure, thermal conductivity and temperature of the fluid respectively.

The significant boundary conditions for the above cases are:

- **for the case of shrinking inner cylinder**

$$\begin{aligned} &r=r_1: u=u_w=-\frac{u_0 x}{l}, v=0, T=T_0;\\ &r=r_2: u=0, T=T_1. \end{aligned} \tag{4}$$

- **for the case of shrinking outer cylinder**

$$\begin{aligned} &r = r_1 : u = 0, v = 0, T = T_0; \\ &r = r_2 : u = u_w = -\frac{u_0 x}{l}, T = T_1. \end{aligned} \tag{5}$$

- **both the cylinders are shrinking**

$$\begin{aligned} &r = r_1 : u = u_w = -\frac{u_0 x}{l}, v = 0, T = T_0; \\ &r = r_2 : u = u_w = -\frac{u_0 x}{l}, T = T_1. \end{aligned} \tag{6}$$

The following similarity transformations [which must satisfy the continuity equation (1)] are adopted to alter the related non-linear governing equations into a new set of solvable systems.

$$\eta = \sqrt{\frac{u_0}{\upsilon l}}\left(\frac{r^2 - r_1^2}{2r_1}\right), \psi = \sqrt{\frac{\upsilon u_0}{l}} r_1 x f(\eta), \theta(\eta) = \frac{T - T_1}{T_0 - T_1}. \tag{7}$$

Implementing the equation (7) into the equations [(2) & (3)], we have achieved the following set of equations:

$$\left(1 + \frac{1}{\beta}\right)\left[(1 + 2\alpha\eta) f''' + 2\alpha f''\right] + f f'' - f'^2 - Ha^2 f' = 0, \tag{8}$$

$$(1 + 2\alpha\eta)\theta'' + 2\alpha\theta' + \Pr f\theta' + \Pr Ec(1 + 2\alpha\eta)\left[1 + \frac{1}{\beta}\right] f''^2 + \Pr EcHa^2 f'^2 = 0. \tag{9}$$

The relevant boundary conditions become:

$$\begin{aligned} &\eta = 0 : f(\eta) = 0, f'(\eta) = -1, \theta(\eta) = 1; \\ &\eta = m : f'(\eta) = 0, \theta(\eta) = 0. \end{aligned} \tag{10}$$

$$\begin{aligned} &\eta = 0 : f(\eta) = 0, f'(\eta) = 0, \theta(\eta) = 1; \\ &\eta = m : f'(\eta) = -1, \theta(\eta) = 0. \end{aligned} \tag{11}$$

$$\begin{aligned} &\eta = 0 : f(\eta) = 0, f'(\eta) = -1, \theta(\eta) = 1; \\ &\eta = m : f'(\eta) = -1, \theta(\eta) = 0. \end{aligned} \tag{12}$$

The boundary conditions [(10)-(12)] represent all the considering cases of this problem. $\alpha = \sqrt{\frac{\upsilon l}{u_0 r_1^2}} = \sqrt{\frac{\upsilon l}{u_0 r_2^2}}, Ha^2 = \frac{\sigma B_0^2 l}{\rho u_0}, \Pr = \frac{\mu C_P}{k} \& Ec = \frac{u_w^2}{C_P T_\infty}$ are the curvature of the cylinders, the

Hartmann number, the Prandtl number and the Eckert number respectively.
The following physical quantities of interest observed in this problem are skin friction coefficient and the Nusselt number that are very important in different physical fields like engineering sciences and geo-physics etc. The quantities are defined as the following way:

$$C_f = \frac{2\mu\left(1+\frac{1}{\beta}\right)}{\rho u_w^2}\left(\frac{\partial u}{\partial r}\right)_{r=R} \& Nu_x = -\frac{Kx}{K(T-T_\infty)}\left(\frac{\partial T}{\partial r}\right)_{r=R}. \tag{13}$$

Using the similarity transformation (7) in (13), we have got the following expression for these quantities:

$$\frac{1}{2} C_f \, \mathrm{Re}_x^{\frac{1}{2}} = \left(1+\frac{1}{\beta}\right) f''(0) \& Nu_x \, \mathrm{Re}_x^{-\frac{1}{2}} = -\alpha\left(1+\frac{1}{\beta}\right)\theta'(0), \tag{14}$$

Where, $\mathrm{Re}_x = \frac{U_0 x^2}{\upsilon l}$ is the local Reynolds number.

2. **Flow Stability:** The flow stability is carried out to distinguish the stable and physically achievable solution. Many researchers (Markin [17], Weidmann *et al. [18]*, etc.) have examined the flow stability and drawn the conclusion that the upper branch (first) solution is stable and physically realizable. To differentiate flow stability of this fluid model, the unsteady form of equations (2) and (3) are considered by adding $\frac{\partial u}{\partial t} \& \frac{\partial T}{\partial t}$ in equations (2) and (3) respectively. The following similarity transformations are utilized to revolutionize the unsteady governing equations into a set of solvable system.

$$\eta = \sqrt{\frac{u_0}{\upsilon l}}\left(\frac{r^2 - r_1^2}{2r_1}\right), \psi = \sqrt{\frac{\upsilon u_0}{l}} r_1 x f(\eta,\tau), \theta(\eta,\tau) = \frac{T-T_1}{T_0-T_1}, \tau = \frac{u_0 t}{l}. \tag{15}$$

Substituting equation (15) into the time dependent flow governing equations, the we have got the subsequent set of equations.

$$\left(1+\frac{1}{\beta}\right)\left[(1+2\alpha\eta)\frac{\partial^3 f}{\partial\eta^3} + 2\alpha\frac{\partial^2 f}{\partial\eta^2}\right] + f(\eta,\tau)\frac{\partial^2 f}{\partial\eta^2} - \left(\frac{\partial f}{\partial\eta}\right)^2 - Ha^2\frac{\partial f}{\partial\eta} - \frac{\partial^2 f}{\partial\eta\partial\tau} = 0, \tag{16}$$

$$(1+2\alpha\eta)\frac{\partial^2\theta}{\partial\eta^2} + 2\alpha\frac{\partial\theta}{\partial\eta} + \Pr f(\eta,\tau)\frac{\partial\theta}{\partial\eta} + \Pr Ec(1+2\alpha\eta)\left[1+\frac{1}{\beta}\right]\left(\frac{\partial^2 f}{\partial\eta^2}\right)^2 + \Pr EcHa^2\left(\frac{\partial f}{\partial\eta}\right)^2 - \Pr\frac{\partial\theta}{\partial\tau} = 0. \tag{17}$$

The associated boundary conditions for this problem are:

$$\begin{aligned}&\eta = 0:\ f(\eta,\tau) = 0, \frac{\partial f}{\partial \tau}(\eta,\tau) = -1, \theta(\eta,\tau) = 1;\\ &\eta = m: \frac{\partial f}{\partial \tau}(\eta,\tau) = 0, \theta(\eta,\tau) = 0.\end{aligned} \tag{18}$$

$$\begin{aligned}&\eta = 0:\ f(\eta,\tau) = 0, \frac{\partial f}{\partial \tau}(\eta,\tau) = 0, \theta(\eta,\tau) = 1;\\ &\eta = m: \frac{\partial f}{\partial \tau}(\eta,\tau) = -1, \theta(\eta,\tau) = 0.\end{aligned} \tag{19}$$

$$\begin{aligned}&\eta = 0:\ f(\eta,\tau) = 0, \frac{\partial f}{\partial \tau}(\eta,\tau) = -1, \theta(\eta,\tau) = 1;\\ &\eta = m: \frac{\partial f}{\partial \tau}(\eta,\tau) = -1, \theta(\eta,\tau) = 0.\end{aligned} \tag{20}$$

For the check of flow stability, the following perturb equations which are taken from Normal Mode Method are considered:

$$\begin{aligned}f(\eta,\tau) &= f_0(\eta) + e^{-\omega\tau} F(\eta,\tau),\\ \theta(\eta,\tau) &= \theta_0(\eta) + e^{-\omega\tau} G(\eta,\tau).\end{aligned} \tag{21}$$

Where, ω is the unknown eigen value parameter. $f_0(\eta)\,\&\,\theta_0(\eta)$ are steady flow solutions and $F(\eta,\tau)\,\&\,G(\eta,\tau)$ small relative to the steady flow solutions which are determined by setting $\tau = 0$ i.e., the small related solutions taken in the forms $F_0(\eta)\,\&\,G_0(\eta)$. Hence $F(\eta,\tau) = F_0(\eta)\,\&\,G(\eta,\tau) = G_0(\eta)$ in equations (16) and (17) reflects the initial decay or growth of the solution of equation (21). In this respect, we have to solve the following linearized eigen value problems which are obtained by Substituting (21) into equations (16) and (17) and used the case $\tau = 0.$

$$\left(1+\frac{1}{\beta}\right)\left[(1+2\alpha\eta)F_0''' + 2\alpha F_0''\right] + \left(f_0 F_0'' + F_0 f_0''\right) - 2 f_0' F_0' - Ha^2 F_0' + \omega F_0' = 0, \tag{22}$$

$$(1+2\alpha\eta)G_0'' + 2\alpha G_0' + \Pr\left(f_0 G_0' + F_0\theta_0'\right) + 2\Pr EC(1+2\alpha\eta)\left[1+\frac{1}{\beta}\right] f_0'' F_0'' + 2\Pr EcHa^2 f_0' F_0' - \Pr\omega G_0 = 0. \tag{23}$$

The boundary conditions became:

$$\begin{aligned}&\eta = 0: F_0(\eta) = 0, F_0'(\eta) = 0, G_0(\eta) = 0;\\ &\eta = m: F_0'(\eta) = 0, G_0(\eta) = 0.\end{aligned} \tag{24}$$

This eigen-value problem gives an infinite set of eigen-values $\omega_1 < \omega_2 < ...,$. The stability of the steady flow solution is based on the least eigen value ω_1.If the least eigen-value $\omega_1 < 0$ then an initial escalation of complexity on the flow is observed and the flow becomes unstable in nature. On the other hand, the positive smallest eigen-value recognizes an initial lie down of disturbances on the flow and it provides stable and achievable flow solution. Following Harish *et al*. [25] and Junoh *et al.* [26], the boundary condition $F_0(0) = 0$ is reduced to $F_0''(0) = 1$ for calculating the eigen-values (ω).

3. **Discussion of the result:** In this study, we have focused on the existence of dual solutions during fluid flow through the annular gap (in the boundary layer region formed in the entrance region) of the concentric cylinders and these exist up to a certain regions of dimensionless similarity variable η. The flow behaviour and the heat transfer phenomena of the Casson fluid motion are discussed graphically for the different flow parameters. Here, the solid lines represent the first solutions, independent of time and the dash lines denote the second solutions, dependent on time. The flow over the shrinking surface helps to form dual solutions. We have discussed the results of this problem in the following cases:

Case 1: When the outer cylinder is stationary with the shrinking inner cylinder of the concentric cylinders:

The impact of the Casson fluid parameter (β) on the fluid motion is shown in Fig. 2. The increasing values of β reduce the viscous force of the fluid which helps to enhance the speed of the fluid during time-independent solution. But, an opposite nature is observed during time dependent solution. Physically, it can be interpreted that at a particular instant of time, the Casson fluid parameter accelerate the fluid motion but with the variation of time, fluid motion experiences retardation with the enhancement of Casson fluid parameter. Also, the temperature of the fluid is reducing with improving values of β [see Fig. 3] during steady case. But, it has the ability to enhance the temperature of the fluid during time dependent case. The curvature parameter helps to accelerate the fluid motion in both the cases (figure 4). From Fig. 5, it is perceived that the curvature parameter helps to reduce the temperature of the fluid motion in both the cases. It is also perceived that the thickness of the thermal boundary layer of the first solution is thicker as compared to the second solution. Physically it can be interpreted that the fluid flow in 2nd case reaches its thermal equilibrium stage sooner than first case. Impacts of Hartmann number (Ha) on velocity and temperature profiles are depicted by Fig. 6 and Fig. 7. Speed of fluid motion diminishes with Ha. The reason behind this phenomenon is that developing values of Ha enhances the resistance of the fluid over the surface and hence the velocity of the fluid enhances. From Fig. 7, it is observed that the Hartmann number (Ha) helps to cool down the fluid motion during both time dependent and independent cases. Thus, the Hartmann number plays an important role to control the thermal transmission of the fluid between the annular region of the cylinders. But, the Eckert number plays a role to enhance the temperature of the fluid during both time-dependent (second solution) and time-independent (first solution) cases [see Fig. 8]. The Eckert number (Ec) is the relation between flow kinetic energy and thermal enthalpy. The kinetic energy enhances for developing values of Ec. Again, it is well known fact that temperature is defined as average kinetic energy, so increasing values of Ec helps to make system warm.

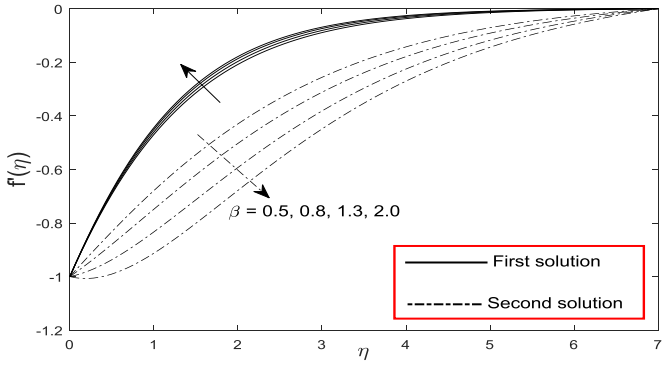

Figure 2: Velocity distribution for incremental values of Casson fluid parameter (β) when $\Pr = 0.71, \alpha = 1, Ha = 0.5, Ec = 0.01$ and inner cylinder is shrinking

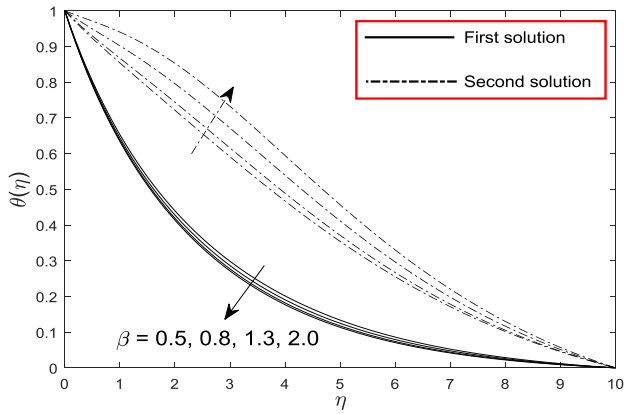

Figure 3: Temperature distribution for incremental values of Casson fluid parameter (β) when $\Pr = 1.7, \alpha = 1, Ha = 0.4, Ec = 0.01$ and inner cylinder is shrinking

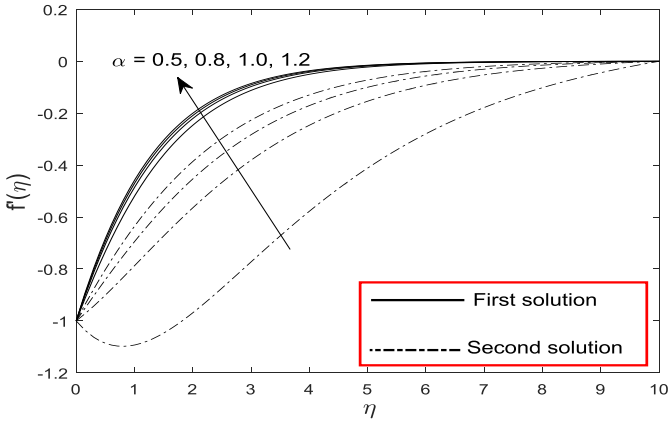

Figure 4: Velocity distribution for incremental values of curvature parameter (α) when $\Pr = 0.71, Ha = 0.4, \beta = 1, Ec = 0.01$ and inner cylinder is shrinking

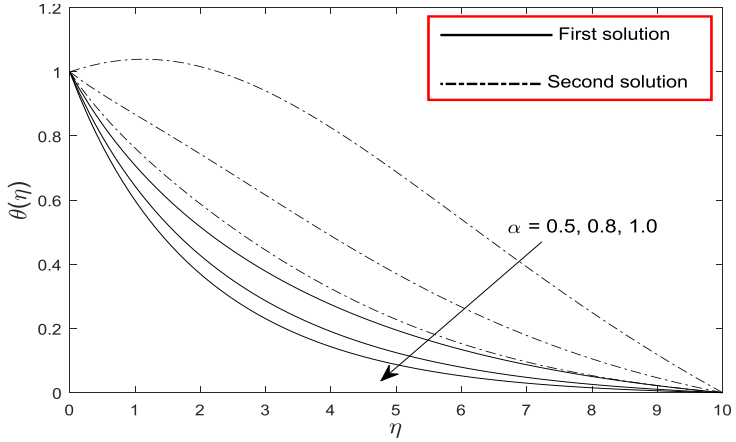

Figure 5: Temperature distribution for incremental values of curvature parameter (α) when $\Pr = 0.71, \beta = 1, Ec = 0.01, Ha = 0.5$ and inner cylinder is shrinking

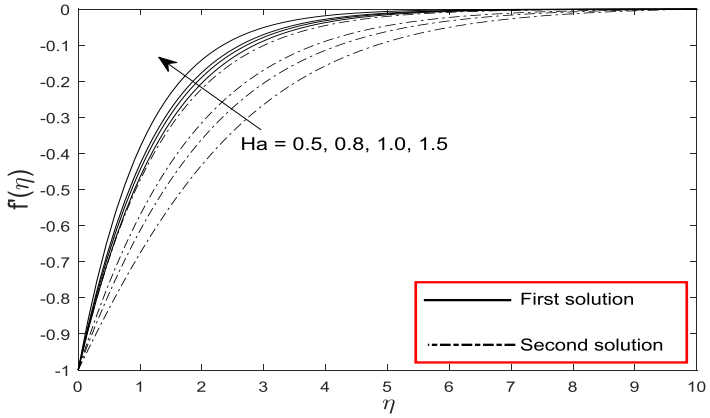

Figure 6: Velocity distribution for incremental values of Hartmann number (Ha) when $\Pr = 0.71, \alpha = 1, \beta = 0.5, Ec = 0.01$ and inner cylinder is shrinking

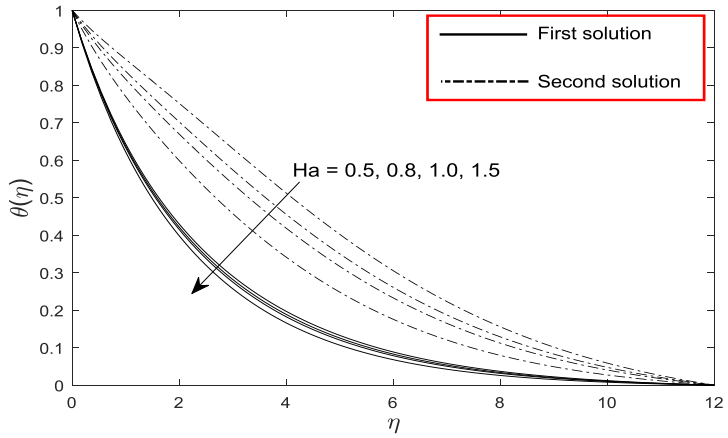

Figure 7: Temperature distribution for incremental values of Hartmann number (Ha) when $\Pr = 1.7, \alpha = 1, \beta = 0.4, Ec = 0.01$ and inner cylinder is shrinking

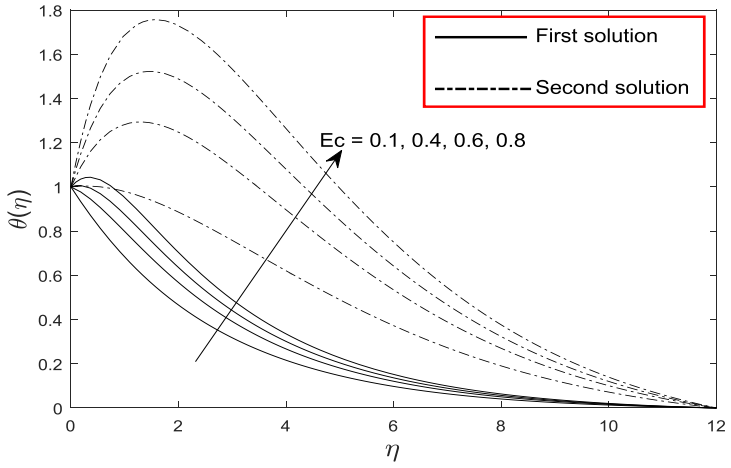

Figure 8: Temperature distribution for incremental values of the Eckert number (Ec) when $\Pr = 1.7, \alpha = 1, \beta = 0.4, Ha = 0.4$ and inner cylinder is shrinking

Case 2: When the inner cylinder is stationary with the shrinking outer cylinder of the concentric cylinders:

The Fig. 9 is depicted to examine the nature of fluid motion for various values of the Casson fluid parameter (β) when the outer cylinder is shrinking. It reflects that the fluid is accelerated in both the cases. Again, it is seen that the fluid motion is accelerated in time independent than the unsteady one. For the temperature distributions of the fluid with Casson fluid parameter (β), is depicted in Fig. 10 and the behaviour confronts with the Fig. 3. Again, growth in curvature parameter of the cylinder helps to control the motion of the fluid during time independent case, but acceleration in fluid motion is seen during time dependent solution [see Fig. 11]. Impact of the curvature of the cylinders on temperature distribution of the Casson fluid is depicted by Fig. 12. From this figure, it is observed that system cools down (during steady and unsteady cases). Thus the parameter helps in controlling the temperature of the system. The figures 13 and 14 are demonstrated to show the influence of the Hartmann number (Ha) on the velocity and temperature fields respectively and the results confronts with the figures 6 and 7 respectively. Again, the influence of the Eckert number (Ec) on the temperature of the fluid for this case [see Fig. 15] is same with the case of shrinking of inner cylinder. It is also seen from Fig. 15 that Eckert number influence on fluid's temperature during time-dependent case (second solution) is more than the first solution.

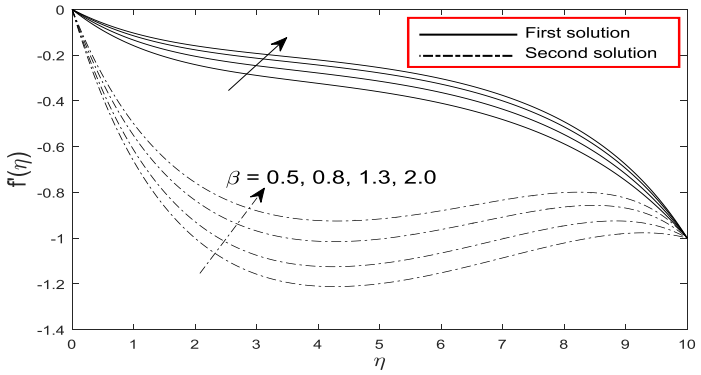

Figure 9: Velocity distribution for incremental values of Cass on fluid parameter (β) when $\Pr = 0.71, \alpha = 1, Ha = 0.5, Ec = 0.01$ and outer cylinder is shrinking

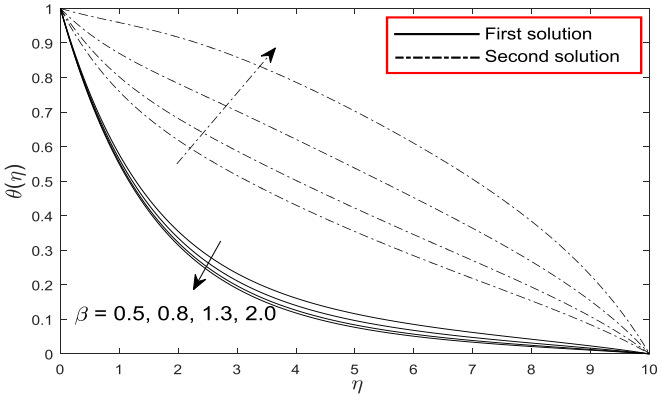

Figure 10: Temperature distribution for incremental values of Casson fluid parameter (β) when $\Pr = 1.7, \alpha = 1, Ha = 0.4, Ec = 0.01$ and outer cylinder is shrinking

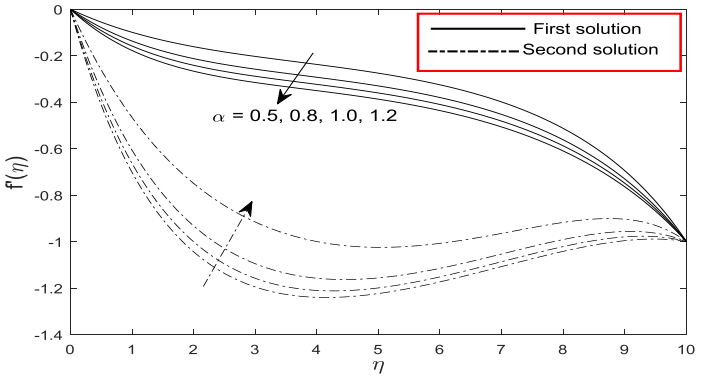

Figure 11: Velocity distribution for incremental values of curvature parameter (α) when $\Pr = 0.71, Ha = 0.4, \beta = 1, Ec = 0.01$ and outer cylinder is shrinking

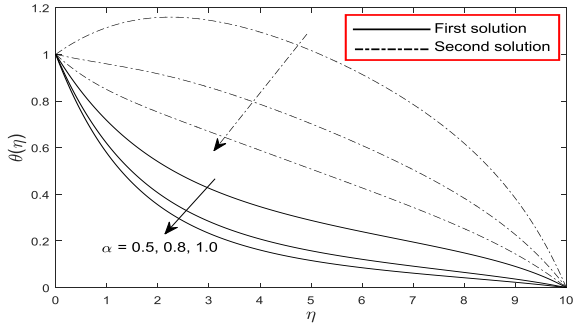

Figure 12: Temperature distribution for incremental values of curvature parameter (α) when $\Pr = 0.71, Ha = 0.4, \beta = 0.5, Ec = 0.01$ and outer cylinder is shrinking

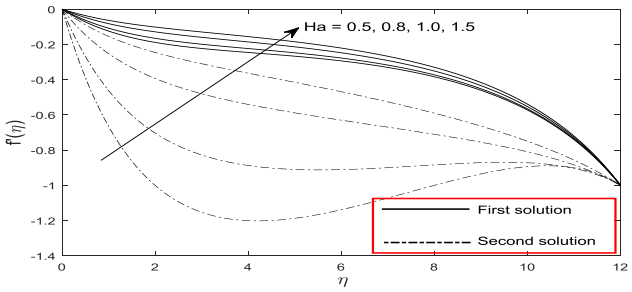

Figure 13: Velocity distribution for incremental values of the Hartmann number (Ha) when $\Pr = 1.7, \alpha = 1, \beta = 0.5, Ec = 0.01$ and outer cylinder is shrinking

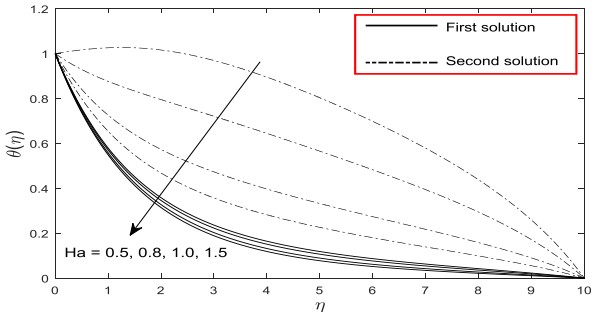

Figure 14: Temperature distribution for incremental values of the Hartmann number (Ha) when $\Pr = 1.7, \alpha = 1, \beta = 0.5, Ec = 0.01$ and outer cylinder is shrinking

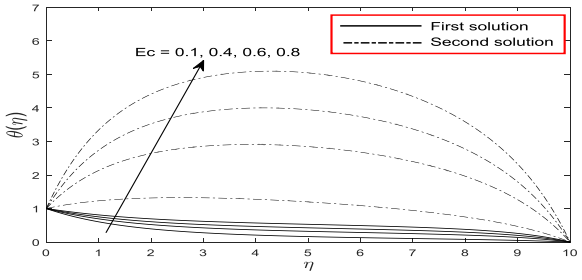

Figure 15: Temperature distribution for incremental values of the Eckert number (Ec) when $\Pr = 1.7, \alpha = 1, \beta = 0.4, Ha = 0.4$ and outer cylinder is shrinking

Case 3: When both the cylinders of the concentric cylinders are shrinking:

The Fig. 16 imitates the velocity of the fluid with β. It is perceived that the velocity of the fluid during steady case is much accelerated than the unsteady case. It can be pointed out that the increasing values of the Cass on fluid parameter (β) accelerate the motion of the fluid during both the cases. But, it is used to protect the system from burning as it helps to reduce the temperature of the system during time independent and time-dependent cases [see Fig. 17]. The Fig. 18 and Fig. 19 reflect the velocity and temperature distributions of the fluid with the improving values of curvature parameter (α). From both the figures, it is noticed that the influence of curvature parameter on the velocity and temperature fields are same with Case-II. The Fig. 20 and Fig. 21 are depicted to show the influence of the Hartmann number (Ha) on the velocity and temperature of the Casson fluid respectively. From these figures, it is perceived that velocity of the fluid during both the solutions accelerate with Ha. The region behind this phenomenon is already discussed in Case-I. The effects of Ha on temperature field of the fluid are remain same with Case-I and Case-II. The influence of Eckert number (Ec) on the temperature of the fluid is demonstrated in Fig. 22. From this figure, we have concluded that the Eckert number is used as enhancement of fluid's temperature. Again, the maximum variation of fluid's temperature is noticed during time-dependent case (second solution) with Ec. The reason behind this physical attribution is already discussed in Case-I and Case-II.

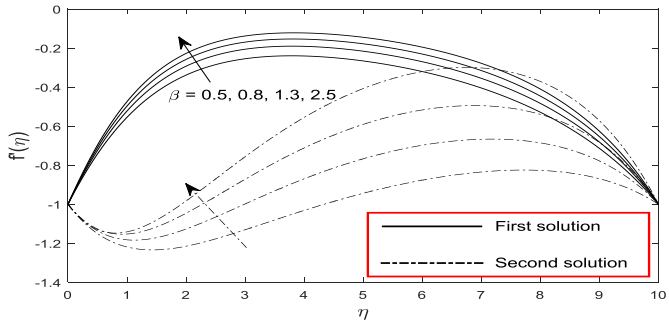

Figure 16: Velocity distribution for incremental values of Casson fluid parameter (β) when $\Pr = 1.7, \alpha = 1, Ha = 0.4, Ec = 0.01$ and both inner and outer cylinders are shrinking

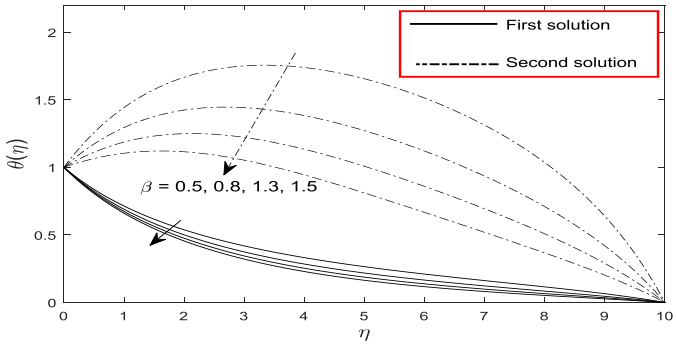

Figure 17: Temperature distribution for incremental values of Casson fluid parameter (β) when $\Pr = 1.7, \alpha = 1, Ha = 0.4, Ec = 0.01$ and both inner and outer cylinders are shrinking

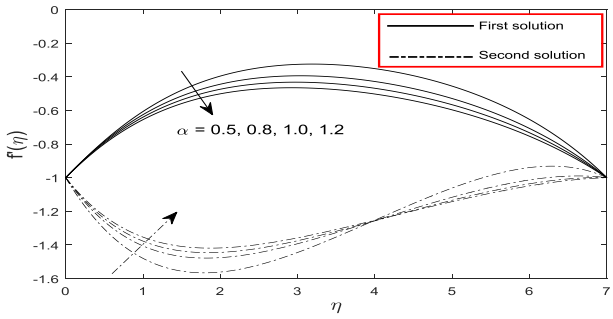

Figure 18: Velocity distribution for incremental values of curvature parameter (α) when $\Pr = 0.71, Ha = 0.4, \beta = 1, Ec = 0.01$ and both inner and outer cylinders are shrinking

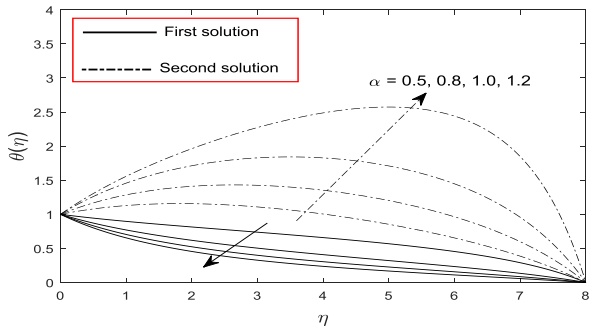

Figure 19: Temperature distribution for incremental values of curvature parameter (α) when $\Pr = 0.71, Ha = 0.4, \beta = 1, Ec = 0.01$ and both inner and outer cylinders are shrinking

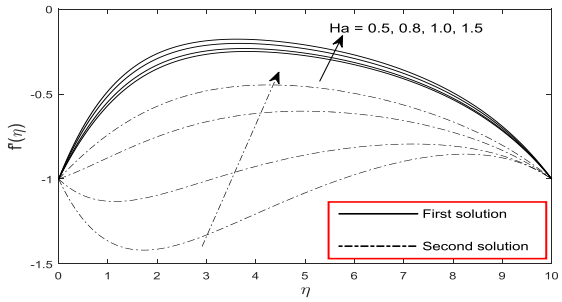

Figure 20: Velocity distribution for incremental values of Hartmann number (Ha) when $\Pr = 1.7, \alpha = 1, \beta = 0.5, Ec = 0.01$ and both inner and outer cylinders are shrinking

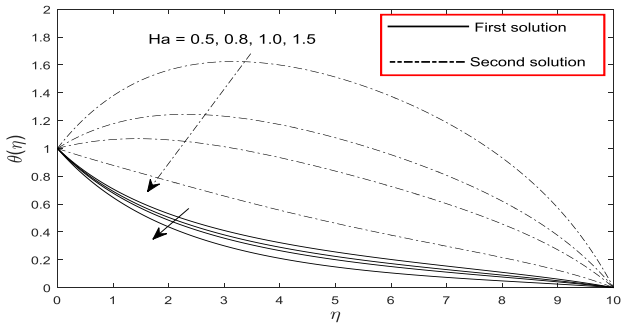

Figure 21: Temperature distribution for incremental values of Hartmann number (Ha) when $\Pr = 1.7, \alpha = 1, \beta = 0.5, Ec = 0.01$ and both inner and outer cylinders are shrinking

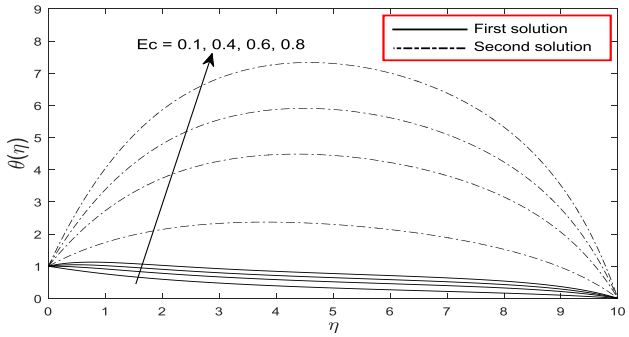

Figure 22: Temperature distribution for incremental values of the Eckert number (Ec) when $\Pr = 1.7, \alpha = 1, \beta = 0.4, Ha = 0.4$ and both inner and outer cylinders are shrinking

All the figures in the above cases visualize the dual solutions of this problem and assure the boundary conditions asymptotically. Again, it is observed that the first solutions appear near the surface of the annular gap and hence it can be achievable practically than the second solutions. The stable and unstable flow solutions are observed in this flow model. To characterise the instability of the dual solutions, a table of smallest eigen values for various values of β is included for the three cases. If the smallest eigen values are happened to be positive then an initial decay of disturbances on the flow is observed and hence the flow become stable. Again, if the least eigen value is found to be negative then the flow will be unstable because it intensifies the initial disturbances on the flow. From the table-1, it is seen that the smallest eigen values for the first solutions are positive for all the cases and hence the first solutions are stable. But, in case of second solution for all the cases, the smallest eigen values are negative and hence an unstable flow is observed during time-dependent case.

Table 1: Numerical values smallest eigen-value (ω) for various values of Cass on fluid parameter when $\Pr = 1.2, Ha = 0.2, \alpha = 1.6, Ec = 0.3$.

	β	Eigen-Value (ω)	
		First Solution	**Second Solution**
First Case (inner cylinder is shrank)	1.0	0.8808	-0.4104
	1.2	0.8731	-0.4132
	1.4	0.8676	-0.4155
Second Case (outer cylinder is shrank)	1.0	0.9496	-0.0021
	1.2	0.9376	-0.0023
	1.4	0.9162	-0.0049
Third Case (inner and outer cylinders are shrank)	1.0	0.9951	-0.0510
	1.2	0.9866	-0.1028
	1.4	0.9844	-0.1554

The physical quantities of interest such as shear stress and rate of heat transfer at the surface are tabulated numerically in Table-2 and Table-3 for all three cases. From the Table-2, it is noticed that the skin friction coefficient of the first solution for the first case enhances but in case of time-dependent solution, it experiences reduction for different values of the

Casson fluid parameter. On the other hand, both the solutions of the skin friction coefficient enhance in all the cases for incremental values of β. A highly impact of the curvature parameter (α) on the skin friction coefficient is observed in Table-2 for all the cases. For the Case-I and Case-III, both the skin frictions (steady and unsteady cases) increases with α. But, it reduces the shear stress at the surface in the second case. Again, the Casson fluid and curvature parameters have a vital role to increase the heat transfer rate at the surface [see Table-3]. That is both the solutions of the Nusselt number for all the cases enhances with different values of $\beta \& \alpha$.

Table- 2: Numerical values of skin friction coefficient for various values of the Casson fluid (β) and curvature (α) parameters when $\Pr = 0.71, Ec = 0.01, Ha = 0.5$.

β	α	**Case-I**		**Case-II**		**Case-III**	
		Skin friction coefficient					
		First solution	Second solution	First solution	Second solution	First solution	Second solution
0.5	1.0	0.7182	0.3524	-0.1735	-0.7062	0.6311	-0.1854
0.8		0.7285	0.2350	-0.1426	-0.6087	0.6675	-0.1531
1.0		0.7330	0.1736	-0.1308	-0.5633	0.6811	-0.1476
1.0	0.5	0.5976	-0.1599	-0.0944	-0.3950	0.5689	-0.2829
	0.8	0.6796	0.2161	-0.1437	-0.6011	0.6168	-0.1845
	1.0	0.7182	0.3524	-0.1735	-0.7062	0.6311	-0.1854

Table- 3: Numerical values of Nusselt number for various values of the Casson fluid (β) and curvature (α) parameters when $\Pr = 0.71, Ec = 0.01, Ha = 0.5$.

β	α	**Case-I**		**Case-II**		**Case-III**	
		Nusselt number					
		First solution	Second solution	First solution	Second solution	First solution	Second solution
0.5	1.0	0.4766	0.1700	0.5977	0.2057	0.3983	-0.4699
0.8		0.4812	0.1520	0.6136	0.3229	0.4286	-0.2658
1.0		0.4833	0.1420	0.6191	0.3639	0.4389	-0.1975
1.0	0.5	0.1619	-0.5790	0.3868	-0.2960	0.3983	-0.4649
	0.8	0.3782	-0.0583	0.5333	0.0396	0.2876	-0.7315
	1.0	0.4766	-0.1700	0.5977	0.2057	0.3983	-0.4699

II. CONCLUSION

The overall conclusions of this investigation are highlighted in the following points:

- From the stability analysis, it is observed that the dual solutions are occurred up to a certain region of the flow direction and the first solutions is stable in manner and physically attainable.
- All the flow parameters for the first case facilitate to enhance the motion of the fluid, but the Casson fluid parameter controls the speed of the fluid during the time

dependent situation. In the case of temperature field of the fluid, all the parameters control the temperature of the fluid, but the Casson fluid parameter has an opposite influence on the time dependent temperature field of the fluid.

- For the second case, the Casson fluid and curvature parameters have the tendency to speed up the fluid, but the curvature parameter plays an important rule because it helps to manage the motion of the fluid.
- The same flow characteristics are seen for the different flow parameters in the third case with the second case.
- Enhancing values of the Eckert number raise the temperature of the fluid in all cases.

III. NOMENCLATURE

β Casson fluid parameter

α curvature parameter

(u_0, l) characteristic velocity (m s^{-1}) and length (m)

ρ density of the fluid (Kg m^{-3})

$f'(\eta)$ dimensionless velocity

$\theta(\eta)$ dimensionless temperature

τ dimensionless time variable

μ dynamic viscosity (Kg m^{-1} s^{-1})

Ec Eckert number

σ electrical conductivity

Ha Hartmann number

υ kinematic viscosity (m^2 s)

Re_x local Reynolds number

Nu_x local Nusselt number

B_0 magnetic field strength (Ns C^{-1} m^{-1})

Pr Prandtl number

μ_B plastic dynamic viscosity

(r_1, r_2) radii of inner and outer cylinders (m)

ψ stream function

(T_0, T_1) surface temperature of the inner and outer cylinders (K)

η similarity variable

C_f skin friction coefficient

C_p specific heat at constant pressure (J Kg^{-1} K^{-1})

T temperature of the fluid (K)

t time (s)

k thermal conductivity (W m^{-1} K^{-1})

ω unknown eigen value

(u, v) velocity along (x, r) directions (m s^{-1})

u_w velocity at surface (m s^{-1})

P_y yield stress"

Reference

[1] L.J. Crane, Flow past a stretching plate, Zeitschrift für Angew. Math. und Phys. ZAMP 21(4): 645–7(1970).

[2] M. Tamoor, M. Waqas, M.I. Khan, A. Alsaedi, T. Hayat, Magnetohydrodynamic flow of Casson fluid over a stretching cylinder, Results Phys 7: 498–502 (2017).

[3] K. Debnath, D. Dey, R. Borah, Thermophoresis and Diffusion Thermo Effects on Shear Thickenning and Shear Thining Cases of Fluid Motion Past a Permeable Surface, J. Mech. Cont. & Mat. Sci 5: 68–81(2020).

[4] D. Dey, M. Hazarika, Entropy Generation of Hydro-Magnetic Stagnation Point Flow of Micropolar Fluid With Energy Transfer Under the Effect of Uniform Suction / Injection, Lat. Am. Appl. Res 50(3): 209–14 (2020).

[5] A. Mahdy, S.E. Ahmed, Unsteady MHD Convective Flow of Non-Newtonian Casson Fluid in the Stagnation Region of an Impulsively Rotating Sphere, J. Aerosp. Eng 30(5): 04017036 (2017).
[6] G. Nagaraju, M. Garvandha, Magnetohydrodynamic viscous fluid flow and heat transfer in a circular pipe under an externally applied constant suction, Heliyon 5(2): 01281 (2019).
[7] Y.H. Krishna, G.V.R Reddy, O.D. Makinde, Chemical reaction effect on MHD flow of casson fluid with porous stretching sheet, Defect Diffus. Forum 389: 100–9 (2018).
[8] .G. Okedayo, E. Enenche, B.I. Obi, A Computational Analysis Of Magneto-Hydrodynamic (MHD) Flow And Heat Transfer In A Cylindrical Pipe Filled With Porous Media 4(7): 89–96 (2017).
[9] I.M. Eldesoky, S.I. Abdelsalam, W.A. El-Askary, A.M. El-Refaey, M.M. Ahmed, Joint Effect of Magnetic Field and Heat Transfer on Particulate Fluid Suspension in a Catheterized Wavy Tube. Bionanoscience 9(3): 723–39 (2019). https://doi.org/10.1007/s12668-019-00651-x
[10] B.J. Gireesha, S. Sindhu, MHD natural convection flow of Casson fluid in an annular microchannel containing porous medium with heat generation/absorption, Nonlinear Eng 9(1): 223–32 (2020).
[11] K, Barman, S. Mothupally, A. Sonejee, P.L. Mills, Fluid Motion Between Rotating Concentric Cylinders Using COMSOL, Multiphysics TM 2–8 (2015).
[12] I.M. Eldesoky, S.I. Abdelsalam, R.M. Abumandour, M.H. Kamel, K. Vafai, Interaction between compressibility and particulate suspension on peristaltically driven flow in planar channel, Appl. Math. Mech 38(1):137–54 (2017). DOI: 10.1007/s10483-017-2156-6
[13] A. Shafee, M. Sheikholeslami, M. Jafaryar, H. Babazadeh, Hybrid nanoparticle swirl flow due to presence of turbulator within a tube, J. Therm. Anal. Calorim no. 0123456789 (2020).
[14] https://doi.org/10.1007/s10973-020-09570-6
[15] S.E. Ahmed, A.K. Hussein, H.A. Mohammed, S. Sivasankaran, Boundary layer flow and heat transfer due to permeable stretching tube in the presence of heat source/sink utilizing nanofluids, Appl. Math. Comput 238: 149–62 (2014). http://dx.doi.org/10.1016/j.amc.2014.03.106
[16] S. Ahmad, M. Ashraf, K. Ali, Simulation of thermal radiation in a micropolar fluid flow through a porous medium between channel walls, J. Therm. Anal. Calorim no. 0123456789 (2020).
[17] https://doi.org/10.1007/s10973-020-09542-w
[18] H. Sadaf, S.I. Abdelsalam, Adverse effects of a hybrid nanofluid in a wavy non-uniform annulus with convective boundary conditions.RSC Adv 10(26): 15035–43 (2020). DOI: 10.1039/d0ra01134g
[19] J.H. Merkin, On dual solutions occurring in mixed convection in a porous medium. J. Eng. Math 20(1): 171–9 (1986).
[20] P.D. Weidmann, A.I.IS. Awaludin, Stability Analysis of Stagnation-Point Flow over a Stretching/Shrinking Sheet, in AIP ADVANCES 045308 (2016).
[21] A. Zaib, K. Bhattacharyya, M.S. Uddin, S. Shafie, Dual Solutions of Non-Newtonian Casson Fluid Flow and Heat Transfer over an Exponentially Permeable Shrinking Sheet with Viscous Dissipation, Model. Simul. Eng. (2016). DOI:10.1155/2016/6968371
[22] N.S.M. Adnan, N.M. Arifin, N. Bachok, F.M. Ali, Stability analysis of MHD flow and heat transfer passing a permeable exponentially shrinking sheet with partial slip and thermal radiation, CFD Lett 11 (12): 34–42 (2019).
[23] A. Ishak, Dual solutions in mixed convection boundary layer flow : A stability analysis, Int. J. Math. , Comput. Phys. Quantum Eng 8(9): 1131–4 (2014).
[24] D. Dey, R. Borah, Dual Solutions of Boundary Layer Flow with Heat and Mass Transfers over an Exponentially Shrinking Cylinder: Stability Analysis, Lat. Am. Appl. Res 50(4): 247–53 (2020).
[25] D. Dey, R. Borah, Stability Analysis on Dual Solutions of Second- grade Fluid flow with Heat and Mass Transfers over a Stretching sheet, Int. J. Thermofluid Sci. Technol 8(2): no. 080203 (2021)
[26] .https://doi.org/10.36963/IJTST.2021080203
[27] G.S. Mishra, M.R. Hussain, O.D. Makinde, S.M. Seth, Stability analysis and dual multiple solutions of a hydromagnetic dissipative flow over a stretching / shrinking sheet. Bulg. Chem. Commun 52(2): 259–71 (2020).
[28] S.D. Harris, ID.B. ngham, I. Pop, Mixed convection boundary-layer flow near the stagnation point on a vertical surface in a porous medium: Brinkman model with slip, Transp. Porous Media, 77(2): 267–85 (2009).
[29] M.M. Junoh, F.M. Ali, N.M. Arifin, N. Bachok, A Stability Analysis of Stagnation-Point Flow of Heat and Mass Transfer over a Shrinking Sheet with Radiation and Slip Effects, Int. J. of Adv. in Sci., Eng. and Technol 6(1):28–32 (2018).

[30] D.R.V.S.R.K. Sastry, Melting and radiation effects on mixed convection boundary layer viscous flow over a vertical plate in presence of homogeneous higher order chemical reaction, Front. Heat Mass Transf 11(3) (2018). DOI: 10.5098/hmt.11.3

[31] D. Dey, B. Chutia, Dusty nanofluid flow with bioconvection past a vertical stretching surface. J. King Saud Univ. - Eng. Sci. (2020). DOI:10.1016/j.jksues.2020.11.001

